AAS 13-804

BROAD-SEARCH ALGORITHMS FOR THE SPACECRAFT TRAJECTORY DESIGN OF CALLISTO-GANYMEDE-IO TRIPLE FLYBY SEQUENCES FROM 2024-2040, PART II: LAMBERT PATHFINDING AND TRAJECTORY SOLUTIONS

Alfred E. Lynam*

Triple-satellite-aided capture employs gravity-assist flybys of three of the Galilean moons of Jupiter in order to decrease the amount of ΔV required to capture a spacecraft into Jupiter orbit. Similarly, triple flybys can be used within a Jupiter satellite tour to rapidly modify the orbital parameters of a Jovicentric orbit, or to increase the number of science flybys. In order to provide a nearly comprehensive search of the solution space of Callisto-Ganymede-Io triple flybys from 2024 to 2040, a third-order, Chebyshev's method variant of the p-iteration solution to Lambert's problem is paired with a second-order, Newton-Raphson method, time of flight iteration solution to the V_∞-matching problem. The iterative solutions of these problems provide the orbital parameters of the Callisto-Ganymede transfer, the Ganymede flyby, and the Ganymede-Io transfer, but the characteristics of the Callisto and Io flybys are unconstrained, so they are permitted to vary in order to produce an even larger number of trajectory solutions. The vast amount of solution data is searched to find the best triple-satellite-aided capture window between 2024 and 2040.

INTRODUCTION

Gravity-assist flybys of planets and moons have been used on several interplanetary missions to reduce the propellant mass and ΔV required to accomplish the missions' objectives. Specifically, the Galileo[1]–[4] and Cassini[5]–[8] missions used gravity-assist flybys of the inner planets to reach their outer planet destinations and performed numerous flybys of the moons of Jupiter and Saturn. The Galileo mission also used an Io gravity assist to reduce the amount of ΔV required to capture into Jupiter orbit by 175 m/s.[3] This concept of using gravity-assist flybys of one or more massive moon to capture a spacecraft into planetary orbit is termed "satellite-aided capture" and has been studied by several investigators.[9]–[21] Triple-satellite-aided capture sequences using Callisto, Ganymede, and Io have the potential to provide trajectory solutions that globally minimize the amount of ΔV required to capture into orbit about Jupiter.[19, 22] Unfortunately, geometric constraints make these triple flyby trajectories difficult to design because they can only occur when Callisto, Ganymede, and Io are properly aligned. While Part I[23] focused on heuristically pruning the solution space using these geometric constraints, this paper concentrates on employing Lambert's problem and V_∞-matching to solve for trajectory solutions within the reduced solution space.

*Assistant Professor, Mechanical and Aerospace Engineering Department, West Virginia University, ESB, Evansdale Dr. Room G-70, Morgantown, WV 26506-6106. Member AIAA. Member AAS.

Lambert's problem is an orbital boundary value problem that involves the calculation of the conic trajectory between two position vectors with a specified time of flight. Numerous investigators[24]–[28] have proposed solutions to this problem, but we employ a third-order, Chebyshev method variant of the p-iteration technique developed by Herrick and Liu[24]. However, the triple flyby problem is not an exact analog to Lambert's problem since only the position vector and flyby time of Ganymede (the second flyby in the triple flyby) are fixed. In order to even pose Lambert's problem in this case, the times of flight of the transfers must coincide with the positions of Callisto and Io before and after the Ganymede flyby. The V_∞- or C3-matching problem must thus be solved in unison with Lambert's problem in order to find the triple flyby solutions. The V_∞- or C3-matching problem has also been investigated in the context of gravity-assist tour design by several authors.[28, 29, 30] In this paper, we employ a second-order, Newton-Raphson method, time of flight iteration solution to the V_∞-matching problem that matches the incoming and outgoing V_∞ of the Ganymede flyby, and ensures that the Ganymede flyby has an altitude of 300 kilometers.

METHODOLOGY

Third-order, Chebyshev-method, p-iteration Lambert solution

Collection of Input Data The first step in the solution process is to extract ephemeris data for Ganymede, Callisto, and Io for the times determined to be feasible from the heuristic pruning in Part I.[23] The first extraction in Part I only extracted the position vectors of the three moons because they were sufficient to find the phase angles between the moons. This second extraction is now necessary because the velocity vectors of the moons are also needed to find the Lambert solutions. In addition to the ephemerides, the initial guesses for $p_{\text{Ca,Ga}}$, $p_{\text{Ga,Io}}$, $T_{\text{Ca,Ga}}$, and $T_{\text{Ga,Io}}$ are extracted from the interpolation structures via the phase angles that were calculated from the ephemerides ($\Delta\lambda_{\text{ephem,Ca,Ga}}$ and $\Delta\lambda_{\text{ephem,Ga,Io}}$). Fig. 1 depicts the Callisto-Ganymede and Ganymede-Io phase angles. In summary, the data inputs to the Lambert-solving and V_∞-matching problem are the time of the Ganymede flyby; the position and velocity vectors of Callisto, Ganymede, and Io at that time; and the initial guesses for the semilatus recta and transfer times of the Callisto-Ganymede and Ganymede-Io orbital transfers ($p_{\text{Ca,Ga}}$, $p_{\text{Ga,Io}}$, $T_{\text{Ca,Ga}}$, and $T_{\text{Ga,Io}}$).

Posing Lambert's problem. In order to find the Lambert solutions, the data inputs first need to be converted into well-posed, orbital two-point boundary value problems. The ephemeris data for Callisto and Io are valid only at the time of the Ganymede flyby, so Callisto's position must be backward-propagated to the time of the Callisto flyby and Io's position must be forward-propagated to the time of the Io flyby. In order to perform the propagations, the mean anomalies of Callisto and Io at the time of the Ganymede flyby are calculated using the position and velocity vectors from the ephemeris data. Next, the mean anomalies of Callisto and Io at their respective flyby times are propagated using the initial guesses for the transfer times ($T_{\text{Ca,Ga}}$ and $T_{\text{Ga,Io}}$):

$$M_{\text{Ca}}(t_{\text{Ca}}) = M_{\text{Ca}}(t_{\text{Ga}}) - n_{\text{Ca}} T_{\text{Ca,Ga}} \tag{1}$$

$$M_{\text{Io}}(t_{\text{Io}}) = M_{\text{Io}}(t_{\text{Ga}}) + n_{\text{Io}} T_{\text{Ga,Io}} \tag{2}$$

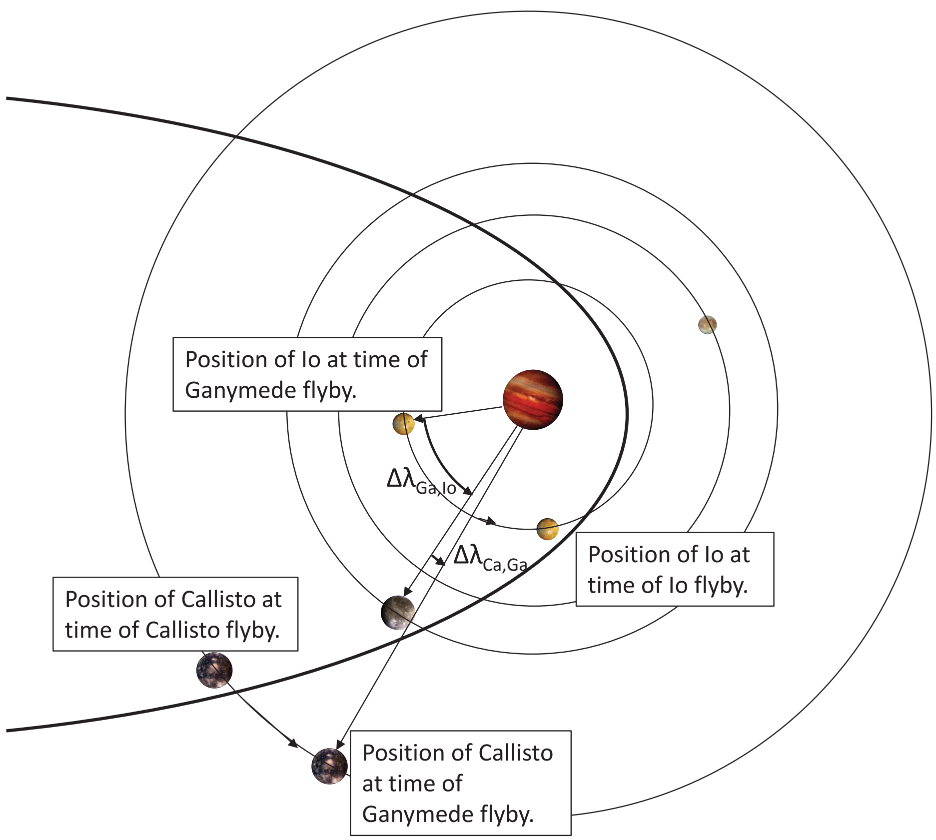

Figure 1. A geometric definition of the Callisto-Ganymede and Ganymede-Io phase angles for a Callisto-Ganymede-Io triple flyby.

where $M_{\text{Ca}}(t_{\text{Ca}})$ and $M_{\text{Io}}(t_{\text{Io}})$ are the mean anomalies of Callisto and Io, respectively, at the times of the spacecraft's flybys of Callisto and Io, respectively, $M_{\text{Ca}}(t_{\text{Ga}})$ and $M_{\text{Io}}(t_{\text{Ga}})$ are the mean anomalies of Callisto and Io at the time of the spacecraft's flyby of Ganymede, and n_{Ca} and n_{Io} are the mean motions of Callisto and Io, respectively. Because Callisto and Io have small orbital eccentricities (0.0074 and 0.0041, respectively), a fifth-order expansion of an equation of the center[31] is used to solve Kepler's equation for the eccentric anomaly propagations in order to avoid iterations.

$$\begin{gathered}
E_{\text{moon}} = M_{\text{moon}} + e_{\text{moon}} \sin M_{\text{moon}} + \tfrac{1}{2} e_{\text{moon}}^2 \sin 2M_{\text{moon}} \\
+\tfrac{1}{8} e_{\text{moon}}^3 \left(3 \sin 3M_{\text{moon}} - \sin M_{\text{moon}}\right) + \tfrac{1}{6} e_{\text{moon}}^4 \left(2 \sin 4M_{\text{moon}} - \sin 2M_{\text{moon}}\right) \\
+\tfrac{1}{384} e_{\text{moon}}^5 \left(125 \sin 5M_{\text{moon}} - 81 \sin 3M_{\text{moon}} + 2 \sin M_{\text{moon}}\right)
\end{gathered}$$

where E_{moon} and M_{moon} are the eccentric and mean anomalies of Callisto or Io at the times of the spacecraft's respective flybys and e_{moon} is the eccentricity of Callisto or Io's orbit about Jupiter. Now that the eccentric anomaly is calculated, the position and velocity vectors of Callisto and Io at the times of the flybys are directly calculated from the eccentric anomaly version of Gauss's f and g functions.[31] Once the propagations using the f and g functions are complete, two Lambert's problems can be posed: the Lambert problem for the Callisto-Ganymede transfer is posed by the Callisto and Ganymede position vectors and the Lambert problem for the Ganymede-Io transfer is posed by the Ganymede and Io position vectors. The initial guesses for the transfer times $T_{\text{Ca,Ga}}$ and $T_{\text{Ga,Io}}$ complete the posing of the two Lambert's problems.

Solving Lambert's problem. Since Lambert's problem is now well posed for both the Callisto-Ganymede transfer and the Ganymede-Io transfer, it can be solved using a variant of the p-iteration technique developed by Herrick and Liu[24] and elaborated on by Bate et al.[32]. As in Bate et al., the semimajor axes of the orbital transfers are calculated from the semilatus rectum guesses $p_{\text{Ca,Ga}}$ and $p_{\text{Ga,Io}}$:

$$a = \frac{mkp}{\left(2m - \ell^2\right) p^2 + 2k\ell p - k^2} \tag{3}$$

where

$$k = r_1 r_2 \left(1 - \cos \Delta\nu\right) \tag{4}$$

$$\ell = r_1 + r_2 \tag{5}$$

$$m = r_1 r_2 \left(1 + \cos \Delta\nu\right) \tag{6}$$

where r_1 is the orbital radius of the first moon in the transfer (Callisto or Ganymede), r_2 is the orbital radius of the second moon in the transfer (Ganymede or Io), and $\Delta\nu$ is the angle between the two radius vectors. Next, we calculate the f and g functions using the true anomaly formulas:

$$f = 1 - r_2 \left(1 - \cos \Delta\nu\right) / p \tag{7}$$

$$g = \frac{r_1 r_2 \sin \Delta\nu}{\sqrt{\mu_{\text{Jup}} p}} \tag{8}$$

$$\dot{f} = \sqrt{\mu_{\text{Jup}}/p} \tan \Delta\nu/2 \left(\frac{1 - \cos \Delta\nu}{p} - \frac{1}{r_1} - \frac{1}{r_2} \right) \tag{9}$$

$$\dot{g} = 1 - r_1 \left(1 - \cos \Delta\nu\right)/p \tag{10}$$

where μ_{Jup} is the gravitational parameter of Jupiter. Since the Callisto-Ganymede and Ganymede-Io orbital transfers could be either elliptical or hyperbolic, the change in either eccentric or hyperbolic anomaly for the transfer is calculated using the following equations:

$$\sin \Delta E = \frac{-r_1 r_2 \dot{f}}{\sqrt{\mu_{\text{Jup}} a}} \tag{11}$$

$$\cos \Delta E = 1 - r_1(1 - f)/a \tag{12}$$

$$\cosh \Delta H = 1 - r_1(1 - f)/a \tag{13}$$

where ΔE is the change in the eccentric anomaly for elliptical transfers and ΔH is the change in the hyperbolic anomaly for hyperbolic transfers. The nominal transfer times associated with the guess values for $p_{\text{Ca,Ga}}$ and $p_{\text{Ga,Io}}$ are calculated next:

$$T_{\text{nom,ellip}} = g + \sqrt{a^3/\mu_{\text{Jup}}} \left(\Delta E - \sin \Delta E\right) \tag{14}$$

$$T_{\text{nom,hyper}} = g + \sqrt{-a^3/\mu_{\text{Jup}}} \left(\sinh \Delta H - \Delta H\right) \tag{15}$$

where $T_{\text{nom,ellip}}$ is the nominal time of flight for an elliptical transfer and $T_{\text{nom,hyper}}$ is the nominal time of flight for a hyperbolic transfer. These nominal times of flight are <u>not</u> in general equal to $T_{\text{Ca,Ga}}$ or $T_{\text{Ga,Io}}$, which is why Lambert's problem requires the iteration of $p_{\text{Ca,Ga}}$ and $p_{\text{Ga,Io}}$ to solve. We use a third-order, Chebyshev's method, p-iteration equation:[33]

$$p_{\text{n+1}} = p_{\text{n}} - \left[1 + \frac{\left(T_{\text{n}} - T_{\text{des}}\right) \partial^2 T_{\text{n}}/\partial p^2}{2\left(\partial T_{\text{n}}/\partial p\right)^2}\right] \tag{16}$$

where $p_{\text{n+1}}$ is the updated value of semilatus rectum, p_{n} is the semilatus rectum of the previous iteration, T_{n} is the nominal time of flight of the previous iteration, T_{des} is the desired time of flight ($T_{\text{Ca,Ga}}$ or $T_{\text{Ga,Io}}$), and $\partial T_{\text{n}}/\partial p$ and $\partial^2 T_{\text{n}}/\partial p^2$ are calculated using central finite differencing:

$$\partial T_{\text{n}}/\partial p = \frac{T(p_{\text{n}} + p_{\text{pert}}) - T(p_{\text{n}} - p_{\text{pert}})}{2p_{\text{pert}}} \tag{17}$$

$$\partial^2 T_{\text{n}}/\partial p^2 = \frac{T(p_{\text{n}} + p_{\text{pert}}) + T(p_{\text{n}} - p_{\text{pert}}) - 2T_{\text{n}}}{p_{\text{pert}}^2} \tag{18}$$

where $T(p_\text{n} + p_\text{pert})$ and $T(p_\text{n} - p_\text{pert})$ are separate propagations of Eqs. 3–15 with semilatus recta perturbed by $\pm p_\text{pert}$. Lambert's problem is solved for the initial guess times of flight when Eq. 16 converges for both transfers:

$$|T(p_\text{Ca,Ga,n}) - T_\text{Ca,Ga}| < tol \tag{19}$$

$$|T(p_\text{Ga,Io,n}) - T_\text{Ga,Io}| < tol \tag{20}$$

where $T(p_\text{Ca,Ga,n})$ and $T(p_\text{Ga,Io,n})$ are the times of flight of the converged semilatus recta and tol is the convergence tolerance.

Newton-Raphson method for V_∞-matching

Although the Lambert solutions for the Callisto-Ganymede and Ganymede-Io transfers are a crucial step in solving the triple flyby problem, there is no mathematical guarantee that the two conic solutions can be patched together. If the incoming Ganymede flyby V_∞ magnitude from the Callisto-Ganymede transfer is not equal to (does not match) the outgoing Ganymede flyby V_∞ magnitude from the Ganymede-Io transfer, then the triple flyby is still impossible even if the two conic trajectories encounter Ganymede at the same time.[29, 30] Even if the incoming and outgoing Ganymede V_∞ magnitudes are equivalent, the angular difference between the incoming and outgoing V_∞ vectors must also be less than the maximum hyperbolic turning angle for a Ganymede flyby at its minimum safe altitude in order for the Ganymede flyby (and thus the triple flyby) to be feasible. These two constraints on the Ganymede flyby parameters can be written in equation form as:

$$F_1 = V^-_{\infty,Ga} - V^+_{\infty,Ga} = 0 \tag{21}$$

$$F_2 = \delta_\text{Ga,max} - \delta_\text{Ga} \geq 0 \tag{22}$$

where F_1 is the V_∞-matching constraint, F_2 is the hyperbolic turning angle constraint, $V^-_{\infty,Ga}$ and $V^+_{\infty,Ga}$ are the incoming and outgoing V_∞ magnitudes of the Ganymede flyby, and

$$\sin \delta_\text{Ga,max}/2 = \frac{1}{1 + (R_\text{Ga} + h_\text{p,Ga,max})(V^-_{\infty,Ga} V^+_{\infty,Ga})/\mu_\text{Ga}} \tag{23}$$

$$\cos \delta_\text{Ga} = \frac{\vec{V}^-_{\infty,Ga} \bullet \vec{V}^+_{\infty,Ga}}{V^-_{\infty,Ga} V^+_{\infty,Ga}} \tag{24}$$

where $\delta_\text{Ga,max}$ is the maximum allowable hyperbolic turning angle for the Ganymede flyby, δ_Ga is the turning angle from the Callisto-Ganymede and Ganymede-Io Lambert solutions, R_Ga is the physical radius of Ganymede, $h_\text{p,Ga,max}$ is the minimum allowable Ganymede flyby altitude, and μ_Ga is the gravitational parameter of Ganymede. The incoming and outgoing V_∞ vectors for the Ganymede flyby are calculated from the Lambert solutions via the f and g functions (Eqs. 7–10) as follows:

$$\vec{V}^-_{\infty,Ga} = (\dot{g}_\text{Ca,Ga} \vec{r}_\text{Ga} - \vec{r}_\text{Ca}) / g_\text{Ca,Ga} - \vec{V}_\text{Ga} \tag{25}$$

$$\vec{V}^+_{\infty,Ga} = (\vec{r}_\text{Io} - f_\text{Ga,Io} \vec{r}_\text{Ga}) / g_\text{Ga,Io} - \vec{V}_\text{Ga} \tag{26}$$

where $g_{\text{Ca,Ga}}$, and $\dot{g}_{\text{Ca,Ga}}$ are f and g functions for the converged Callisto-Ganymede transfer, $f_{\text{Ga,Io}}$ and $g_{\text{Ga,Io}}$ are f and g functions for the converged Ganymede-Io transfer, $\vec{r}_{\text{Ca}}$, $\vec{r}_{\text{Ga}}$, and $\vec{r}_{\text{Io}}$ are the converged position vectors of the moons from the Lambert solutions, and $\vec{V}_{\text{Ga}}$ is the velocity vector of Ganymede from the ephemerides.

The constraint equation for F_1 (Eq. 21) matches the incoming and outgoing Ganymede flyby V_∞ and is in a suitable form for use in an iterative, multidimensional, Newton-Raphson root-solving algorithm. However, the equation for F_2 (Eq. 22) is an inequality constraint, so it must be converted into an equality constraint to be solved using the Newton-Raphson method. One method of converting the inequality constraint into an equality constraint would be to introduce a slack variable and then find a minimum norm solution. However, we chose to assume that the mission designer would always want the maximum possible hyperbolic turning angle for the Ganymede flyby. Thus, we simply replaced the $\geq$ sign in Eq. 22 with an $=$ sign:

$$F_2 = \delta_{\text{Ga,max}} - \delta_{\text{Ga}} = 0 \tag{27}$$

Since we now have two equality constraints, multidimensional root solving requires the iteration of two design variables. Since we have extracted initial guesses for the transfer times $T_{\text{Ca,Ga}}$ and $T_{\text{Ga,Io}}$ from the interpolation structures developed in Part I[23], those two parameters are used as design variables in a Newton-Raphson, multidimensional root solving algorithm. In summary, the constraint vector ($\bar{F}$) and the design variable vector ($\bar{X}$) are given by the following equations:

$$\bar{F} = \begin{pmatrix} F_2 \\ F_1 \end{pmatrix} \tag{28}$$

$$\bar{X} = \begin{pmatrix} T_{\text{Ca,Ga}} \\ T_{\text{Ga,Io}} \end{pmatrix} \tag{29}$$

The equation that updates the times of flight $T_{\text{Ca,Ga}}$ and $T_{\text{Ga,Io}}$ to satisfy the constraint equations is:

$$\bar{X}^{\text{j}+1} = \bar{X}^{\text{j}} - \left(\frac{\partial \bar{F}}{\partial \bar{X}}\right)^{-1} \bar{\text{F}}(\bar{X}^{\text{j}}) \tag{30}$$

where $\left(\partial \bar{F} / \partial \bar{X}\right)$ is the Jacobian matrix of the system and is calculated via central finite differencing with equations similar to Eq. 17. The convergence criteria for the V_∞-matching algorithm are similar to those in Eqs. 19 and 20. For each iteration, the design variables are changed, so Lambert's problem must be solved again to find the Callisto-Ganymede and Ganymede-Io transfers consistent with the new times of flight. Thus, the V_∞-matching process is the iterative outer loop that solves for the Ganymede flyby conditions and the Lambert solution process is the iterative inner loop that solves for the Callisto-Ganymede and Ganymede-Io transfers. Fig. 2 depicts the V_∞-matching process.

Calculating the Callisto and Io Flybys: Mission Design Considerations

The combined V_∞-matching and Lambert problem only calculates the Ganymede flyby conditions, the Callisto-Ganymede and Ganymede-Io transfers, and the Jupiter-centered positions of the Callisto and Io flybys. Hence, the Callisto and Io flyby conditions are not yet specified. While there

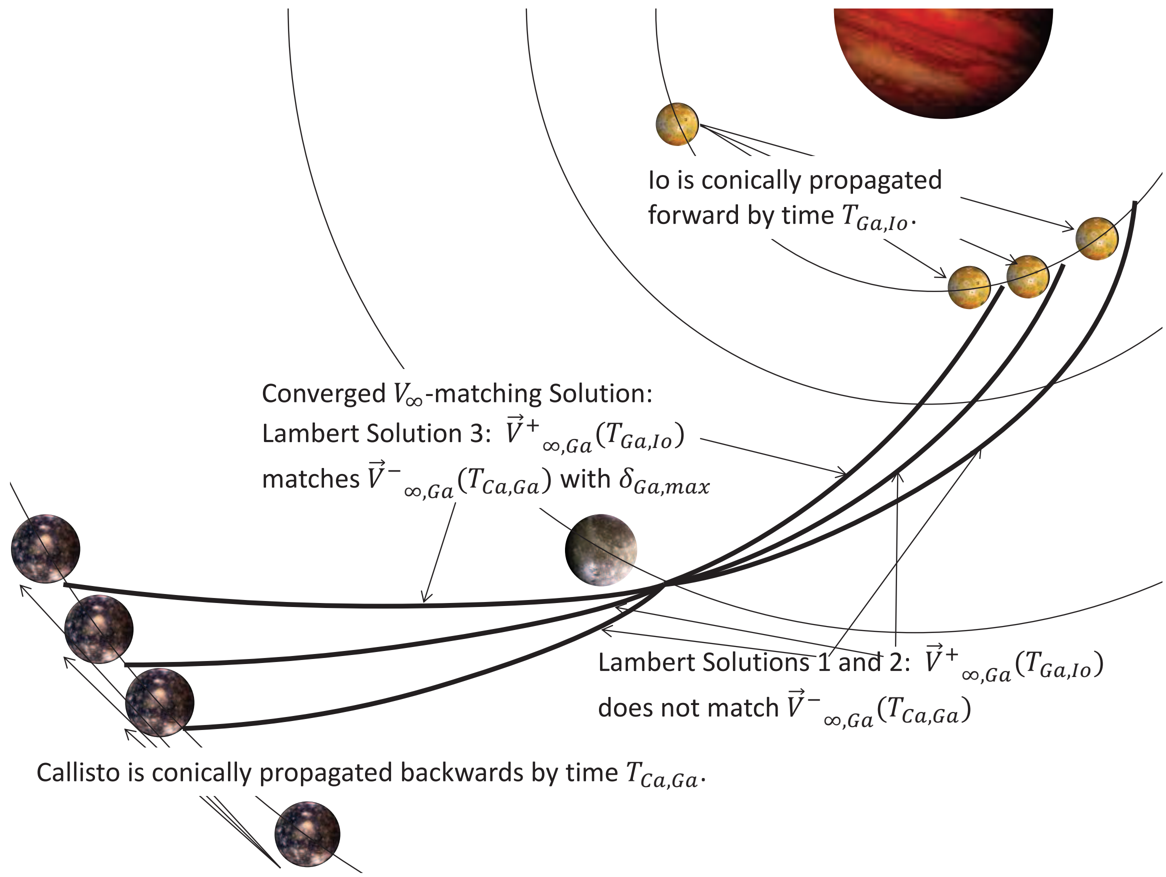

Figure 2. Within the V_∞-matching process, Lambert's problem is solved iteratively. The convergence criteria for the V_∞-matching problem are that the incoming V_∞ at Ganymede from a converged Callisto-Ganymede transfer Lambert solution matches the outgoing V_∞ at Ganymede from a converged Ganymede-Io transfer Lambert solution with a specified hyperbolic turning angle for the Ganymede flyby ($\delta_{\mathbf{Ga,max}}$).

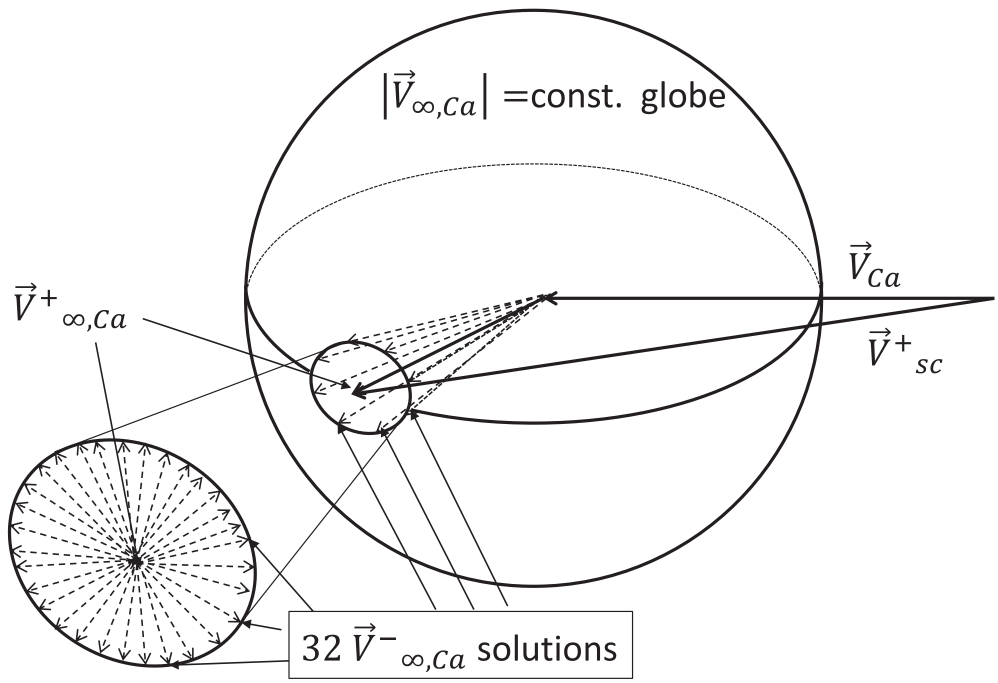

Figure 3. Globe of constant V_∞ for Callisto Flyby. The post-flyby V_∞ is fixed, but there are 32 possible solutions for the pre-flyby V_∞ on the "small circle" surrounding the post-flyby V_∞ on the V_∞-globe.

are an infinite number of possible Callisto and Io flybys at the beginning and end of a triple flyby sequence, we limit that solution space by specifying the hyperbolic turning angles of the flybys as the maximum safe turning angles (corresponding to the minimum safe flyby altitudes). These hyperbolic turning angles are calculated using analogous equations to Eq. 23. Combining the V_∞-globe terminology of Strange et al.[34] with the terminology of cartography, the solution space for the Callisto and Io flybys are "small circles" on the Callisto and Io V_∞-globes which are centered around the outgoing Callisto V_∞ vector and the incoming Io V_∞ vector. These "small circles" are discretized into 32 equally-spaced flyby solutions for both the Callisto and Io flyby as depicted by Fig. 3. While this discretization technically generates 1024 trajectories for each triple flyby solution, only 64 need to be recorded since the mission design after the triple flyby is distinct from the mission design before the flyby sequence. Before this point, the problem was a purely computational astrodynamics problem to solve for triple flybys. Now, practical mission design considerations need to be taken into account in order to select which 2 of the 64 possible trajectories to consider further.

From a mission design standpoint, there are three practical uses for triple flybys. Triple flybys could be used to capture a spacecraft into orbit about Jupiter, to allow a spacecraft to escape Jupiter orbit, or to be used within a Jupiter satellite tour as science flybys. For the third case, the 32 pre-Callisto solutions would be used to connect the triple flyby to the earlier stages of the satellite tour.

Similarly, the 32 post-Io solutions would be used to connect the triple flyby to the remainder of the tour. The full incorporation of triple flybys into Jupiter satellite tours is beyond the scope of this paper, but a plausible method of incorporation would be to connect the pre-Callisto and post-Io apojoves with apojoves from other orbits in the tour. The capture and escape cases are dynamically symmetric, so only the capture case will be discussed in detail. Some of the limited mission design uses of a Jupiter escape would be for Europa sample returns or multi-planet satellite tours. In contrast, all Jupiter satellite tour missions would require capture, so triple flybys for capture (i.e. triple-satellite-aided captures) would be useful for a wide range of Jupiter mission scenarios.

The most efficient triple-satellite-aided captures occur when the Io and Callisto flybys are equatorial flybys that maximally reduce the Jupiter-centered orbital energy of the orbit. Thus, the post-Io solution that minimizes Jupiter-centered orbital energy should always be chosen for an optimal capture. Since the Callisto flyby is modeled in the negative time direction, the pre-Callisto solution that maximizes Jupiter-centered orbital energy before the Callisto flyby should be chosen for an optimal capture. These guidelines inform the choice of the trajectories before and after the triple-satellite-aided capture sequence.

RESULTS

Mission Design of Triple-satellite-aided Capture Sequences

After the best pre-Callisto and post-Io trajectories are chosen for each of the calculated triple flybys, there are still thousands of possible triple flybys in the solution space to investigate for triple-satellite-aided capture sequences. Obviously, the Ganymede flyby should be energy-reducing rather than energy-increasing for a capture, which eliminates about 1/2 of the remaining solution space. The final mission design consideration is finding a feasible Earth/Mars to Jupiter transfer before the Callisto flyby. This consideration requires that the incoming Jupiter-centered V_∞ vector be as close to anti-parallel as possible with Jupiter's heliocentric velocity vector.

$$180^\circ - \cos^{-1}\left[\frac{\vec{V}^-_{\infty,\text{Jup}} \bullet \vec{V}_{\text{Jup,Sun}}}{\left|\vec{V}^-_{\infty,\text{Jup}}\right| \left|\vec{V}_{\text{Jup,Sun}}\right|}\right] \approx 0^\circ \tag{31}$$

where $\vec{V}^-_{\infty,\text{Jup}}$ is the spacecraft's incoming, Jupiter-centered V_∞ vector and $\vec{V}_{\text{Jup,Sun}}$ is Jupiter's heliocentric velocity vector. $\vec{V}_{\text{Jup,Sun}}$ is estimated from ephemeris data for the Ganymede flyby times of the triple flybys, and $\vec{V}^-_{\infty,\text{Jup}}$ is calculated for all 32 pre-Callisto solutions for all triple flyby solutions that have hyperbolic pre-Callisto trajectories. This calculation is performed for both Callisto-Ganymede-Io-Perijove triple flybys (that have three flybys in a row and then pass perijove) and Callisto-Ganymede-Perijove-Io triple flybys (that have two flybys of Callisto and Ganymede, pass perijove, and then perform a flyby of Io). The angle results for Callisto-Ganymede-Io-Perijove (CGIP) triple flybys are plotted in Fig. 4. The thick lines represent available, backward-propagated optimal transfers to the inner solar system at 2026 and 2033. These two trajectory windows will later be searched using STK to determine if an ideal Earth-Jupiter or Mars-Jupiter transfer is available.

Similarly, the angle results for Callisto-Ganymede-Perijove-Io (CGPI) triple flybys are plotted in Fig. 5. There are more available CGPI trajectories than CGIP trajectories because there about three times as many triple flybys in Part I[23] that had Io flybys after perijove than those that had Io flybys before perijove. A total of nine trajectory windows will be searched in STK for CGPI trajectories: two in 2026 and one in 2029, 2030, 2033, 2034, 2036, 2037, and 2039.

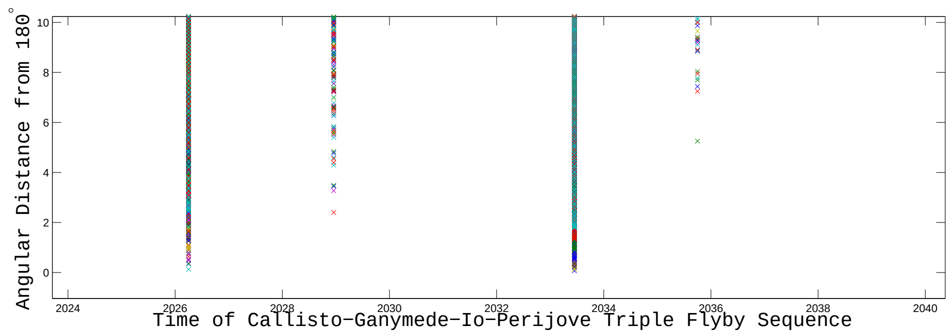

Figure 4. For Callisto-Ganymede-Io-Perijove triple flybys, there are two possible, backward-propagated optimal transfers to the inner solar system: at 2026 and at 2033 (thick lines).

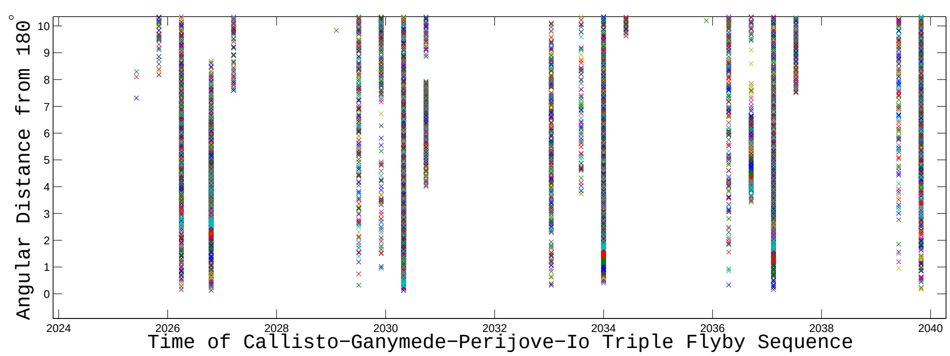

Figure 5. For Callisto-Ganymede-Perijove-Io triple flybys, there are nine possible, backward-propagated optimal transfers to the inner solar system (some of the lines).

Table 1. **Characteristics of the Six Feasible Trajectory Windows.**

Trajectory Window (Ganymede Flyby)	Arrival V_∞	Capture Orbit	Flybys
CGIP April 2 2026	4.7 km/s	590 days	Earth Flyby
CGIP June 14 2033	5.1 km/s	509 days	Mars Flyby
CGPI April 2 2026	5.3 km/s	587 days	Earth Flyby
CGPI Dec. 2 2029	3.6 km/s	97 days	Mars Flyby
CGPI Jan. 15 2033	5.7 km/s	2933 days	Mars Flyby
CGPI Dec. 31 2034	5.7 km/s	Hyperbolic	Earth and Mars

High-fidelity Triple-Satellite-Aided Captures in STK

High-fidelity, triple-satellite-aided capture trajectories were computed in STK for each of the 11 CGIP and CGPI trajectory windows. A series of two nested targeting loops were used to target the B-plane parameters of the Callisto, Ganymede, and Io flybys. The STK targeting methodology used was similar to that used by Lynam et al.[19, 20] to target double- and triple-satellite-aided capture sequences. After the triple-satellite-aided capture sequences were found, they were backward-propagated for 2 or 3 years until they reached the inner solar system. For five of the trajectory windows, Earth and Mars flybys were both unavailable because of poor phasing (the second 2026 CGPI trajectory, the 2030 CGPI trajectory, the 2036 CGPI trajectory, the 2037 CGPI trajectory, and the 2039 CGPI trajectory). Thus, there are six feasible trajectory windows for CGIP and CGPI trajectories between 2024–2040; several features of these six trajectory windows are described in Table 1.

In Table 1, the sequence type (CGIP vs. CGPI) and the month and year of Jupiter arrival are listed in the first column for all six feasible trajectory windows. In the second and third columns, the arrival V_∞ of the spacecraft at Jupiter and the capture orbit period after the triple flybys (assuming no impulsive ΔV) are given. The first three trajectories have capture orbit periods between 500 and 600 days, so they would require impulsive ΔV's at perijove (Jupiter orbit insertion maneuvers) of about 100 m/s to reduce their capture orbit periods to 200 days (the capture orbit of Galileo[4]) and about 200 m/s to reduce their capture orbit periods to 100 days. The fourth trajectory has a capture orbit period of 97 days, so it does not require chemical propulsion to capture into Jupiter orbit. The fifth and six trajectories do not capture into feasible capture orbits, so an impulsive ΔV of 225 m/s would be required to capture them into 200-day orbits and 350 m/s for 100-day orbits. These impulsive JOI ΔV estimates are based on the methodology of Lynam et al.[19]

On the fourth column of Table 1, possible flybys of Earth or Mars are listed for each trajectory window. Unlike the double-satellite-aided capture trajectories of Lynam and Longuski[20] that had precise, ballistically-propagated, backward-targeted flybys of Earth, these triple-satellite-aided capture trajectories would miss Earth by millions of kilometers without additional ΔV applied between Earth and Jupiter. This miss distance is due to the fact that Jupiter arrival V_∞ is the only available control variable after triple-satellite-aided capture sequences are targeted, and the B-planes for Earth and Mars flybys have two target variables: $B \bullet R$ and $B \bullet T$. Because the ballistic backward-targeting problem is overconstrained, additional ΔV is required to backward-target the

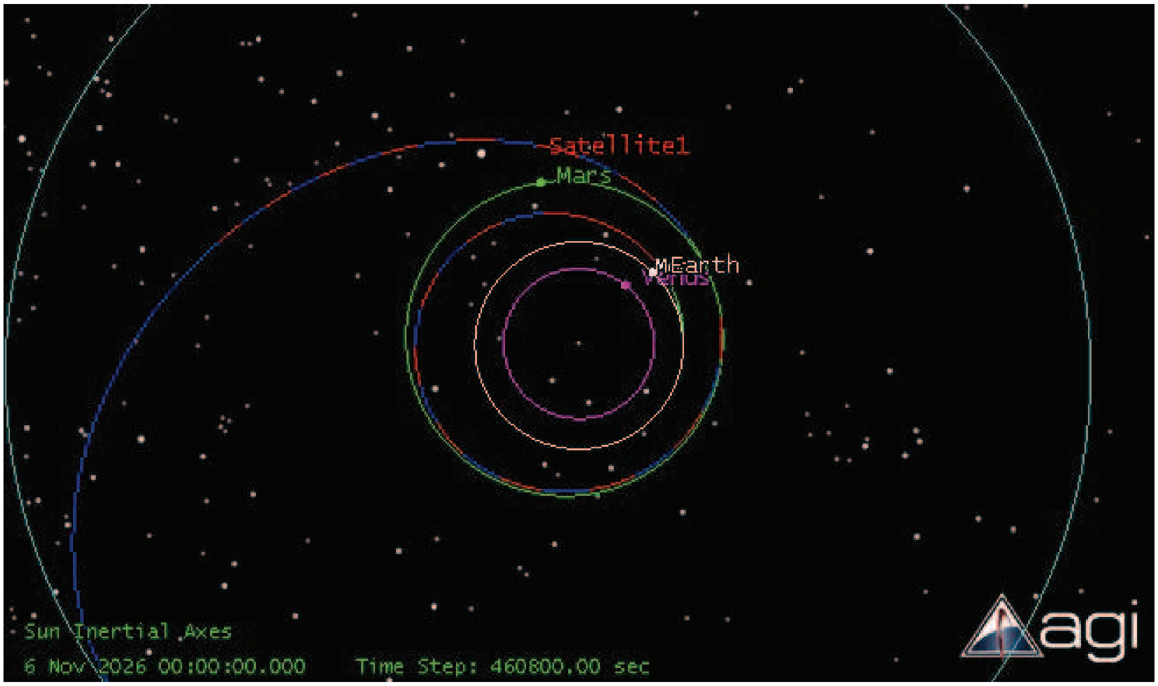

Figure 6. Interplanetary, low-thrust trajectory in STK that launches from Earth on September 2024, flys by Mars on May 2026, and arrives at Jupiter on December 2029.

Earth or Mars flybys. Although it is possible to use chemical propulsion to provide enough ΔV to backward-target the Earth or Mars flybys, the additional impulsive ΔV (which would translate into extra required chemical propellant mass) would defeat the purpose of using triple-satellite-aided capture vs. double-satellite-aided capture, which is to save additional propellant mass. Hence, we suggest that low-thrust, Solar electric propulsion (SEP) trajectories similar to those discovered by Landau et al.[17] and Strange et al.[18] be used for the heliocentric portion of the trajectories.

Because the CGPI Dec. 2029 is the only trajectory that is feasible with only low-thrust, solar electric propulsion and would not require a chemical Jupiter orbit insertion maneuver, we focus on finding a full trajectory from Earth launch to Mars flyby to Jupiter triple-satellite-aided capture for that window only. Because STK does not have a low-thrust trajectory optimizer, we approximate low-thrust by adding impulsive maneuvers at 30-day increments along the cruise from Earth to Mars and from Mars to Jupiter. In Fig. 6, the spacecraft launches from Earth, performs several simulated low-thrust maneuvers (indicated by the switches between blue and red in the trajectory plot), flys by Mars, performs several more simulated low-thrust maneuvers, and coasts to Jupiter once it is far enough away from the Sun that Solar electric propulsion would be less useful. The low-thrust maneuvers are primarily in the velocity direction, but they have slight normal and co-normal (out-of-plane) components to backward target the Mars flyby and Earth launch. The time of flight of the converged trajectory from Earth to Jupiter capture is 5.2 years, the total amount of unoptimized low-thrust ΔV is 7.3 km/s, and the maximum required low-thrust acceleration is about 2×10^{-7} $\mathrm{km/s^2}$ (which corresponds to a thrust of 1 Newton for a 5000 kg spacecraft).

The Callisto-Ganymede-Perijove-Io capture sequence at Jupiter is plotted on Fig. 7. The spacecraft performs a flyby of Callisto, transfers to a Ganymede flyby 19 hours later, passes its perijove at 4.2 R_{J} 17 hours later, performs a flyby of Io 4 hours later, and captures into a 97-day capture orbit.

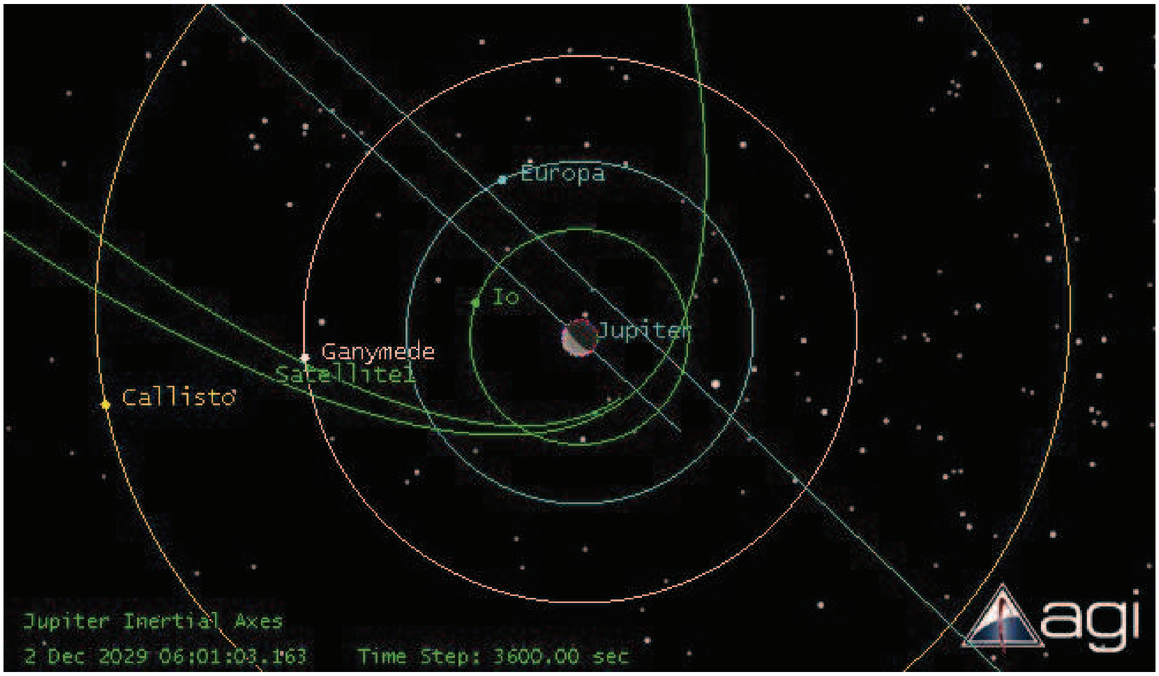

Figure 7. A Callisto-Ganymede-perijove-Io triple-satellite-aided capture sequence is used to ballistically capture a spacecraft into a 97-day orbit.

Since the goal is to reduce the capture orbit period as much as physically possible, all three of the flybys had low flyby altitudes: the Callisto flyby had an altitude of 95 km, the Ganymede flyby had an altitude of 125 km, and the Io flyby had an altiude of 137 km. These low altitude flybys in rapid succession would require precise and rapid navigation, perhaps even autonomous navigation.[21] It would be straightforward to find higher altitude flybys for this trajectory window at the cost of longer capture orbit periods.

DISCUSSION

A vast number of triple flyby solutions were computed using second-order, p-iteration Lambert solving and V_∞-matching. In retrospect, the p-iteration Lambert solver was probably not the best option, because it has a singularity for 180° transfers. The triple flyby solutions had constrained Ganymede flybys, but their Callisto and Io flybys were unconstrained, so the solution spaces of the Callisto and Io flybys were discretized into 32 different pre-Callisto and 32 different post-Io solutions for each triple flyby. The hyperbolic pre-Callisto solutions were backward propagated via f and g functions to estimate the Jupiter-centered arrival V_∞ vectors. The angles between these arrival V_∞ vectors and the concurrent heliocentric velocity vectors of Jupiter were calculated for all hyperbolic pre-Callisto solutions. The hyperbolic pre-Callisto solutions that had angles near 180° were further investigated within STK. Eleven trajectory windows were searched within STK, and six of these trajectory windows (recorded in Table 1) had feasible backward targeted Earth or Mars flybys.

In Table 1, the CGPI Dec. 2029 trajectory window is the best because the spacecraft's capture orbit is less than 100 days without any additional impulsive ΔV. Thus, a spacecraft using a low-thrust, solar electric propulsion (SEP) system could capture into orbit about Jupiter using this trajectory without having an additional chemical propulsion system. This triple-satellite-aided capture trajectory is qualitatively similar to the Callisto-Perijove-Ganymede (CPG) double-satellite-aided capture trajectory found by Strange et al.[18] that would arrive at Jupiter in June 2027. The notable differences between the CGPI Dec. 2029 trajectory and the CPG June 2027 trajectory found by Strange et al. are that the capture orbit period is much lower for the CGPI trajectory (97 days vs. 354 days), the CGPI trajectory would be more difficult to navigate[21], the CGPI trajectory has a lower perijove (4.2 R_{J} vs. 9.4 R_{J}) so it would accumulate more radiation[35], and there is only one CGPI trajectory with these characteristics between 2024 and 2040 whereas there are likely several CPG trajectories with these characteristics, since it is much more common for two moons to geometrically align for flybys than three. The primary advantages of having a shorter capture orbit period are that less propellant and thrust would be required to mitigate solar perturbations and that the spacecraft would be able to begin its primary science mission sooner rather than spend a long time in a capture orbit.

While the other five triple-satellite-aided capture windows in Table 1 would be physically feasible, they are likely less optimal than CPG double-satellite-aided capture because they would require either more chemical ΔV to backward target the Mars or Earth flybys or require the awkward construction of a spacecraft with both chemical and electric propulsion. The other five solutions would also have the same navigation and radiation difficulties as the more optimal CGPI Dec. 2029 solution. It is possible that other Callisto, Ganymede, and Io triple flybys with different flyby orders (e.g. a Ganymede flyby, then an Io flyby, and then a Callisto flyby after perijove) may produce other optimal trajectories that are similar to the CGPI Dec. 2029 solution, but for now that solution is the only solution that would compare favorably with double flybys.

CONCLUSIONS

A nested Lambert and V_∞-matching solver was used to find numerous Callisto-Ganymede-Io triple flybys from the candidate trajectory times from Part I[23]. These triple flybys were post-processed to find optimal triple flybys for triple-satellite-aided capture for missions to Jupiter. One particularly attractive Lambert solution was transformed into a fully integrated, end-to-end, low-thrust trajectory from Earth to Jupiter capture. This trajectory solution would launch from Earth in September 2024, perform a gravity assist of Mars, and arrive at Jupiter in December 2029. Upon Jupiter arrival, the spacecraft would capture into a 97-day orbit about Jupiter after performing gravity-assist flybys of Callisto, Ganymede, and Io. The benefits of using this particular trajectory over other triple flyby and double flyby solutions are that chemical propulsion is not needed to capture the spacecraft into a feasible capture orbit and the capture orbit period is much shorter than alternative solutions. This shorter capture orbit would allow the spacecraft to begin its science mission sooner and reduce the propellant cost required to mitigate solar perturbations. Although this trajectory was integrated but not optimized, it is likely that an optimized variant of this solution may provide a trajectory that optimally balances the goals of maximizing payload mass and minimizing time of flight for a Jupiter science mission.

REFERENCES

[1] C. Potts and M. Wilson, "Maneuver Design for the Galileo VEEGA Trajectory," *AAS Paper 93-566, Proceedings of the AAS/AIAA Astrodynamics Specialist Conference*, Victoria, B.C., Canada, Aug. 1993.

[2] T. Barber, F. Krug, and B. Froidevaux, "Initial Galileo Propulsion System In-Flight Characterization," *AIAA Paper No: 93-2117, Proceedings of the AIAA/SAE/ASME/ASEE 29th Joint Propulsion Conference and Exhibit*, Monterrey, CA, June 1993.

[3] M. G. Wilson, C. L. Potts, R. A. Mase, C. A. Halsell, and D. V. Byrnes, "Manuever Design for Galileo Jupiter Approach and Orbital Operations," *Space Flight Dynamics, Proceedings of the 12th International Symposium*, Darmstadt, Germany, June 1997, pp. 1–9.

[4] R. Haw, P. Antreasian, T. McElrath, and G. Lewis, "Galileo Prime Mission Navigation," *Journal of Spacecraft and Rockets*, Vol. 39, 2000, pp. 56–63.

[5] T. D. Goodson, D. L. Gray, Y. Hahn, and F. Peralta, "Cassini Maneuver Experience: Finishing Inner Cruise," *AAS Paper 00-167, Proceedings of the AAS/AIAA Spaceflight Mechanics Meeting*, Clearwater, FL, January 2000.

[6] D. Roth, P. Antreasian, J. Bordi, K. Criddle, R. Ionasescu, R. Jacobson, J. Jones, M. C. Meed, I. Roundhill, and J. Stauch, "Cassini Orbit Reconstruction from Jupiter to Saturn," *AAS Paper 05-311, Proceedings of the AAS/AIAA Astrodynamics Specialist Conference*, Lake Tahoe, CA, August 2005.

[7] P. N. Williams, C. G. Ballard, E. M. Gist, T. D. Goodson, Y. Hahn, P. W. Stumpf, and S. V. Wagner, "Flight Path Control Design for the Cassini Equinox Mission," *Proceedings of the AAS Spaceflight Mechanics Meeting*, Savannah, GA, February 2009.

[8] C. G. Ballard, J. Arrieta, Y. Hahn, P. W. Stumpf, S. V. Wagner, and P. N. Williams, "Cassini Maneuver Experience: Ending the Equinox Mission," *AIAA Paper 2010-8257, AIAA/AAS Astrodynamics Specialists Conference*, Toronto, ON, CA, August 2010.

[9] R. W. Longman, "Gravity Assist from Jupiter's Moons for Jupiter-Orbiting Space Missions," tech. rep., The RAND Corp., Santa Monica, CA, 1968.

[10] R. W. Longman and A. M. Schneider, "Use of Jupiter's Moons for Gravity Assist," *Journal of Spacecraft and Rockets*, Vol. 7, No. 5, May 1970, pp. 570–576.

[11] J. K. Cline, "Satellite Aided Capture," *Celestial Mechanics*, Vol. 19, May 1979, pp. 405–415.

[12] K. T. Nock and C. Uphoff, "Satellite Aided Orbit Capture," *AAS Paper 79-165, Proceedings of the AAS/AIAA Astrodynamics Specialist Conference*, Provincetown, MA, June 25–27, 1979.

[13] J. R. Johannesen and L. A. D'Amario, "Europa Orbiter Mission Trajectory Design," *AAS Paper 99-330, Proceedings of the AAS/AIAA Astrodynamics Conference*, Vol. 103, Girdwood, AK, August 1999.

[14] M. Malcolm and C. McInnes, "Spacecraft Planetary Capture Using Gravity-Assist Maneuvers," *Journal of Guidance, Control, and Dynamics*, Vol. 28, March-April 2005, pp. 365–368.

[15] C. H. Yam, *Design of Missions to the Outer Planets and Optimization of Low-Thrust, Gravity-Assist Trajectories via Reduced Parameterization*. PhD thesis, School of Aeronautics and Astronautics, Purdue University, West Lafayette, IN, May 2008, pp. 96–104.

[16] M. Okutsu, C. H. Yam, and J. M. Longuski, "Cassini End-of-Life Escape Trajectories to the Outer Planets," *AAS Paper 07-258, Proceedings of the AAS/AIAA Astrodynamics Specialist Conference*, Mackinac Island, MI, August 2007.

[17] D. Landau, N. Strange, and T. Lam, "Solar Electric Propulsion with Satellite Flyby for Jovian Capture," *Proceedings of the AAS/AIAA Spaceflight Mechanics Conference*, San Diego, CA, February 2010.

[18] N. Strange, D. Landau, R. Hofer, J. Snyder, T. Randolph, S. Campagnola, J. Szabo, and B. Pote, "Solar Electric Propulsion Gravity-Assist Tours For Jupiter Missions," *AIAA Paper No: 2012-4518, Proceedings of the AIAA/AAS Astrodynamics Specialists Conference*, Minneapolis, MN, August 2012.

[19] A. E. Lynam, K. W. Kloster, and J. M. Longuski, "Multiple-satellite-aided Capture Trajectories at Jupiter using the Laplace Resonance," *Celestial Mechanics and Dynamical Astronomy*, Vol. 109, No. 1, 2011.

[20] A. E. Lynam and J. M. Longuski, "Interplanetary Trajectories for Multiple Satellite-Aided Capture at Jupiter," *Journal of Guidance, Control, and Dynamics*, Vol. 34, No. 5, September-October 2011.

[21] A. E. Lynam and J. M. Longuski, "Preliminary Analysis for the Navigation of Multiple-satellite-aided Capture Sequences at Jupiter," *Acta Astronautica*, 2012.

[22] A. E. Lynam, K. W. Kloster, and J. M. Longuski, "An Assessment of Multiple Satellite-Aided Capture at Jupiter," *AAS Paper 09-424, Proceedings of the AAS/AIAA Astrodynamics Specialists Conference*, Pittsburgh, PA, August 2009.

[23] A. Lynam, "Broad-search Algorithms for the Spacecraft Trajectory Design of Callisto-Ganymede-Io Triple Flyby Sequences from 2024-2040, Part I: Heuristic Pruning of the Search Space," *Proceedings of the AAS/AIAA Astrodynamics Specialists Conference*, Hilton Head, SC, August 2013.

[24] S. Herrick and A. Liu, "Appendix A: Two Body Orbital Determination from Two Positions and Time of Flight," *Aeronutronic*, Vol. C-365, 1959.

[25] E. Lancaster, R. Blanchard, and R. Devaney, "A Note on Lambert's Theorem," *Journal of Spacecraft and Rockets*, Vol. 3, 1966, pp. 1436–1438.

[26] R. Gooding, "A Procedure for the Solution of Lambert's Orbital Boundary-Value Problem," *Celestial Mechanics and Dynamical Astronomy*, Vol. 48, 1990, pp. 145–165.

[27] R. Battin, *An Introduction to the Mathematics and Methods of Astrodynamics*. Reston, VA: AIAA, 1999.

[28] N. Anora and R. Russell, "A GPU Accelerated Multiple Revolution Lambert Solver for Fast Mission Design," *AAS Paper No: 10-198, Proceedings of the AAS/AIAA Spaceflight Mechanics Meeting*, San Diego, CA, February 2010.

[29] S. Williams, *Automated Design of Multiple Encounter Gravity-Assist Trajectories*. West Lafayette, IN: M.S. Thesis, Purdue University, 1990.

[30] J. Longuski and S. Williams, "Automated Design of Gravity-Assist Trajectories to Mars and the Outer Planets," *Celestial Mechanics and Dynamical Astronomy*, Vol. 52, 1991, pp. 207–220.

[31] D. Vallado, *Fundamentals of Astrodynamics and Applications, 3rd edition*. New York, NY: Springer, 2007.

[32] R. Bate, D. Mueller, and J. White, *Fundamentals of Astrodynamics*. New York, NY: Dover Publications, 1971.

[33] S. Amat, S. Busquier, and J. Gutierrez, "Geometric Constructions of Iterative Functions to Solve Nonlinear Equations," *Journal of Computational and Applied Mathematics*, Vol. 157, 2003, pp. 197–205.

[34] N. Strange, R. Russell, and B. Buffington, "Mapping the V-infinity Globe," *AAS Paper No: 07-277, Proceedings of the AAS/AIAA Astrodynamics Specialists Conference*, Mackinac Island, MI, August 2007.

[35] K. Kloster, A. Petropoulos, and J. Longuski, "Europa Orbiter Tour Design with Io Gravity Assists," *Acta Astronautica*, Vol. 68, 2010, pp. 931–946.